Non-stoichiometry effect and disorder in Cu_2ZnSnS_4 thin films obtained by flash evaporation: Raman scattering investigation

R. Caballero[1,*], E. Garcia-Llamas[1,2], J.M. Merino[1], M. León[1], I. Babichuk[3], V. Dzhagan[3], V. Strelchuk[3], M. Valakh[3].

[1]Universidad Autónoma de Madrid, Departamento de Física Aplicada, C/ Francisco Tomás y Valiente 7, E-28049 Madrid, Spain

[2]Helmholtz-Zentrum Berlin für Materialien und Energie, Hahn-Maitner-Platz 1, D-14109 Berlin, Germany

[3]V. Lashkaryov Institute of Semiconductor Physics of National Academy of Sciences of Ukraine, 41 Prospect Nauky, 03028 Kyiv, Ukraine

Abstract

The cation disorder in Cu_2ZnSnS_4 thin films grown by flash evaporation of ZnS, CuS and SnS binary compounds has been studied by Raman spectroscopy. Process parameters such as the substrate temperature during the evaporation and the Ar-pressure in the post-thermal treatment determined the samples composition and Raman spectra. As a measure of cation disorder, the half-width and relative intensity of the Raman band peaked at 331-332 cm^{-1} is analysed. Comparison of the spectra for different samples of known composition showed that the relative intensity of the defect peak 331 cm^{-1} correlates with the previously reported theoretical prediction about enhancement of antisite defect formation in CZTS under "Cu-poor, Zn-rich" conditions. For films of "Cu-rich, Zn-poor" composition, further experimental confirmation was obtained of the previously detected effect of the enhancement of cation disorder under intense optical excitation.

Keywords: Cu_2ZnSnS_4, solar cells, cation disorder, non-stoichiometry, Raman scattering, flash evaporation.

*Corresponding author. Tel.: +34 91 497 8559; fax: +34 91 497 3969

E-mail address: raquel.caballero@uam.es (R. Caballero)

1. Introduction

Recently Cu_2ZnSnS_4 (CZTS) and similar quaternary chalcogenides have received considerable attention as potential materials for thin film solar cells of new generation. The reasons are their suitable direct band gap energy of about 1.5 eV, large optical absorption coefficient of 10^4 - 10^5 cm^{-1}, and the fact that all constituents of CZTS are abundant in the crust of the earth, non-expensive and non-toxic. During last decade the efficiency of CZTSSe-based solar cells has been improved significantly and reached 11.1% [1-3].

The efficiency of application of CZTS in photovoltaics is determined substantially by its structural features. This compound can be formed in two crystallographic structures: kesterite (KS) (space group $I\bar{4}$) and stannite (ST) (space group $I\bar{4}2m$) [2]. The kesterite structure possesses lower formation energy. However, as far as the binding energy difference between KS and ST is small (3 meV/atom according to calculations) [2, 3], the subject of numerous experimental works published up to now has been to determine the real structure of the samples obtained by different methods. It has been shown experimentally that CZTS usually crystallizes in the kesterite structure, but the problem is that the latter may contain a very high concentration of intrinsic defects related with non-stoichiometry in the cation sublattice [4]. The proximity of the properties of Cu and Zn atoms reduces significantly the efficiency of traditional X-ray diffraction to investigate this problem. In particular, a reliable identification of antisite-defects such

as Cu_{Zn} and Zn_{Cu}, which essentially define the electrical characteristics of the samples, requires more expensive techniques such neutron scattering and synchrotron radiation [5-9]. The dominance of different sorts of intrinsic defects in CZTS prepared by different methods is not only an interesting fundamental problem, but also a crucial application issue. It is known that the defects formed under Cu-poor and Zn-rich growth conditions of CZTS should be beneficial for the solar cell performance [1].

The problem of non-stoichiometry in crystalline CZTS samples obtained by Bridgman method and solid-state reaction of pure elements has been studied by means of Raman spectroscopy in our previous reports [10-12]. This issue was also discussed for CZTS films grown by pneumatic spray pyrolysis in [13]. The disordering of the cation sublattice for non-stoichiometry (Cu-poor, Zn-rich)-type CZTS material has been accompanied by the appearance of a new Raman band at about 331 cm^{-1}. This band has properties of A-mode and is observed either simultaneously with or instead of the A-mode of the "normal" (i.e. ordered) kesterite, peaked at 338 cm^{-1} [10-12]. The structure with significant concentration of Cu-Zn antisite defects is called disordered kesterite [8, 9] and is characterized by a change of the symmetry of the crystal lattice from $I\bar{4}$ to $I\bar{4}2m$ (the latter being the same as in stannite).

In this paper, we investigate the structure of CZTS thin films, obtained by flash evaporation, by Raman spectroscopy. A relationship between the spectral Raman features and growth conditions of CZTS films and their composition is established.

2. Experimental details

CZTS thin films were deposited by flash evaporation of ZnS, CuS and SnS binary compounds in powder form onto molybdenum-coated glass substrates at a nominal substrate temperature, T_{sub}, of 100º C or 350º C. The CuS and SnS powders used were synthesized in an evacuated quartz ampoule from the pure elemental constituents, while

commercially available ZnS was used. A preferential re-evaporation of Zn has been observed during the flash evaporation process independent of the evaporation source used. It is related to a preferential Zn re-evaporation due to its high partial vapor pressure [14]. Because of that, a precursor with excess of ZnS was used in our deposition procedure. Table I summarizes the growth conditions and final chemical composition of as-evaporated thin films. As shown in Table I, the precursor with a ZnS excess > 15 % is necessary to achieve the atomic ratio of [Zn]/[Sn] > 1 which has been previously shown to be necessary for high efficiency CZTS-based solar cells [1]. The composition was measured by Energy Dispersive X-ray spectroscopy (EDX) (Oxford instruments, model INCAx-sight) of a Hitachi S-3000N scanning electron microscope. EDX measurements were carried out at 20 kV operating voltage and included Cu K, Zn K, Sn L and S K lines. It can be seen from Table I that thin film composition depends on the crucible temperature during evaporation, $T_{crucible}$. Lower crucible temperatures lead to higher Cu concentrations (samples F19 and F20). A substoichiometric CuS content was used for deposition of samples F26 and F27. The lower CuS content is important when the evaporation is carried out at higher substrate temperature because of an enhanced Cu incorporation at increaseing T_{sub}. The first experiment was carried out at T_{sub} = 100º C (sample F26) and no significant change in the Cu concentration was observed. In spite of a 10% less CuS content than required for a stoichiometric compound, the resulting [Cu]/([Zn]+[Sn]) atomic ratio is still very high for the sample F27 grown at substrate temperature of 350º C.

The evaporated samples were annealed in Ar atmosphere (P=100 or 1000 Pa) in a partially closed graphite container placed inside a quartz tube furnace. 20 mg of elemental sulfur was placed into the graphite box prior to heating. Variations of annealing temperature as well as of annealing times at maximum temperature were investigated in order to obtain a single phase CZTS thin film material (see Table II).

Heating rates from 10 to 21º C/min were used for the thermal treatments, and the samples were cooled down naturally. The importance of the Ar pressure is demonstrated by the different composition obtained after applying the thermal treatments 1 and 2.

Micro-Raman spectroscopy study was performed in backscattering configuration with a T64000 Horiba-Jobin-Ivon spectrometer by using the 514.5 nm excitation wavelength of an Ar^+-ion laser. Laser radiation with power I_o < 1 mW was focused with a 50x objective to spot about 1 μm on the sample. Due to non-uniformity of some films surface, visible under the light microscope, Raman spectra were measured in different areas of each sample.

3. Results

3.1. As-evaporated films.

The typical spectra of as-evaporated thin films deposited on the substrate heated up to 100° C are shown in Figure 1. In the spectral range of 150-450 cm^{-1} up to five Raman bands usually appear with frequencies of about 251, 287, 331, 353, and 363 cm^{-1}. All these frequencies, except for 331 cm^{-1}, are practically the same (within ± 3cm^{-1}) as the phonon frequencies of CZTS bulk crystals and films with kesterite structure [10-12, 15-17]. The only difference is the larger (2-2.5 times) half-width of the bands in our work. It is related to the no so crystalline structure for the samples evaporated at only T_{sub} = 100° C. The main band at 331 cm^{-1} observed in Figure 1 can be the A-symmetry mode of kesterite CZTS, which is shifted downwards due to the disorder in cationic sublattice. This assignment is based on our recent finding of the relation between the presence of the 331 cm^{-1} peak and significant disorder in the cation sublattice of the kesterite, initiated by the non-stoichiometry of the cationic composition – [Cu]/([Zn] + [Sn]) < 1 [10-12]. Such a type of non-stoichiometry takes place for all the films

deposited at T_{sub} = 100^{o} C with the exception of the sample F19, for which [Cu]/([Zn] + [Sn]) ≈ 1 (see Table I). We believe that the reason for this fact is that at low T_{sub} the no stoichiometric films grow with high concentration of Cu_{Zn} and Zn_{Cu} antisite defects due to the similar sizes of Cu and Zn cations.

Figure 2 shows the Raman spectrum of the sample F27 evaporated at nominal substrate temperature of 350º C. A critical effect of the substrate temperature is clearly observed. In this case the spectrum is very the same as for the ordered CZTS, with intense and narrow (Γ= 4.9 cm^{-1}) A-peak at 339.3 cm^{-1}. A small upward shift of A-peak with respect to the more typical value of 338 cm^{-1} can be induced by residual compressive strain in the CZTS film due to different temperature expansion coefficients of the Mo/glass substrate and CZTS film.

3.2. Annealed films.

Table II shows the composition of the samples after different annealing treatments. The thermal treatment of the films evaporated at T_{sub} = 100º C lead to the transformation of their wide spectra to relatively narrow dominant A-peak at 338 cm^{-1}, which is typical for kesterite structure. As is expected, after the thermal treatment the crystalline quality of these samples is strongly enhanced. For all the samples, the broad band of disordered kesterite at 331-332 cm^{-1} disappeared after annealing. This fact correlates with the EDX data (see Table II), which shows that mainly none of the annealed samples reveal typical chemical composition for the disordered kesterite structure, i.e. Cu-poor and Zn-rich [11].

Figure 3 displays the Raman spectrum of the annealed sample-F27 at 475º C for 60 min at P_{Ar} = 100 Pa. For this case the Cu-rich and Zn-poor composition was obtained, that is the composition predicted theoretically to be optimal for the formation of the ordered kesterite structure [3, 9]. Raman spectrum of the annealed sample-F20 at 600º C for 30

min at P_{Ar} = 1000 Pa is shown in Figure 4. In this case, the condition “Cu poor” is achieved which is known to stimulate the effect of cation disorder in kesterite. Here, a larger half-width of the A-peak corresponding to the ordered kesterite is obtained compared with all other samples.

4. Discussion

The effect of non-stoichiometry on the degree of disorder and parameters of "defect" Raman band at 331 cm^{-1} can be seen from comparing the width of the 331 cm^{-1} band, Γ_{331}, for samples F20 and F24 before annealing. According to the theoretical prediction in [7, 9] and direct experimental results of [6], the formation of defects in CZTS is stimulated by (Cu-poor, Zn-rich)-type deviation from stoichiometry. Therefore, based on the composition of samples F20 and F24 (see Table I), more disorder could be expected for the sample F20 because of a larger value of Γ_{331}. Indeed, Γ_{331}=34 cm^{-1} for sample F20 while for sample F24 Γ_{331}=30 cm^{-1} (see Figure 1).

The degree of disorder of the kesterite structure can be estimated from the Raman spectra based on the intensity ratio of the peak at 332 cm^{-1} to that of the peak 338 cm^{-1}, I_{332}/I_{338}, for the samples after annealing. It turned out that among all the investigated samples the smallest I_{332}/I_{338} value was measured for the sample F27 (see Table III), thus confirming the theoretical prediction in [3]. As mentioned above, only for sample F20 annealed at 600° C and P_{Ar} =1000 Pa for 30 min the condition “Cu-poor” is achieved. Despite the fact that for this sample the Zn content is close to the stoichiometric content (rather than Zn-rich), the half-width of A-peak for this sample is noticeably larger (6.1 cm^{-1}) compared with all other samples (e.g. 3.9 cm^{-1} for F27). Beside the position of A-peak is shifted down by 1 cm^{-1} from the value corresponding to the ordered kesterite, 338 cm^{-1} (Figure 4), the peak at 287 cm^{-1} is significantly broader and weak in intensity.

It seems that the number of Cu^{+} vacancies in this CZTS sample is large enough to stimulate lattice disordering. In the case of excess of Zn^{2+}-ions, this can result in a change of symmetry of crystalline structure due to the formation of Zn_{Cu} antisites [3, 11].

By comparing the samples with similar content of Cu and Zn (F27(-) and F27(3), F24(1) and F19(1)) (the number in bracket indicates the thermal treatment applied), we first evaluate the accuracy of the relationship between Raman spectra and cation composition of CZTS. As can be seen from Table III, the values of the I_{332}/I_{338} ratio for the latter two pairs do not differ more than 20%. Thus, for the subsequent establishing of the relationship between the I_{332}/I_{338} ratio and cation composition of CZTS, we should take into account only the changes in I_{332}/I_{338} which are sufficiently larger than 20%.

A comparison of all the spectra of the annealed samples and full analysis of Table III allow us to draw some preliminary conclusions about the relationship between Raman spectra and cation composition of CZTS. For this purpose, we compare the spectra of samples with similar content of one of the components (Cu or Zn) and significantly different content of another component (Zn or Cu). As can be seen from Table III, it is possible to choose four pairs of samples: F27(3) and F19(1), F19(2) and F20(1), F19(2) and F20(2), F19(1) and F20(1). For three of the four mentioned pairs of samples, the ratio I_{332}/I_{338} increases as the Zn content changes from “poor“ to “stoichiometric” and then to “rich” (at almost constant Cu content). The same trend in the I_{332}/I_{338} ratio is observed for the samples with close Zn content and Cu content changing from “rich” to “stoichiometric” and to “poor“. This result is completely consistent with the theoretically predicted criteria of the stability of (ordered) kesterite structure – “Cu-rich, Zn-poor” [3, 6, 9]. The exception from this trend can be found by the pair of samples F19(1) and F20(1). Here the I_{332}/I_{338} ratio is 20% larger for Cu-rich sample

(F19(1)) than for Cu-stoichiometric sample (F20(1)), for the same Zn content. However, this exception is within the estimated experimental error of 20 %. For the other three pairs of samples analyzed above, the difference of I_{332}/I_{338} ratio was much more pronounced: 44% for samples F19(2) and F20(2), 67% for samples F19(2) and F20(1), and 300% for samples F27(3) and F19(1). Therefore, we can conclude that the relative intensity of the 332 cm^{-1} band can be used for assessment of the degree of the cation disorder in kesterite structure. This can be further illustrated in Figure 5. This Figure shows the Raman spectrum of the sample F27(3) measured at four times higher laser light power than that used for the spectrum in Figure 3. Earlier, we have shown that intense optical excitation of CZTS-crystal with composition "Cu-rich, Zn-poor" can induce disordering in the cation sublattice, if the radiation stimulates the transition in cation subsystem from a state of Cu^{+} to Cu^{2+} (the latter is more typical for copper) [18]. Such a transition is accompanied by a decrease of the size of the copper ion from 96 pm to 72 pm. The last is practically the same as the size of the Zn^{2+}-ion (74 pm). As a result, the probability of forming Cu_{Zn} antisite defects increases significantly. As can be seen from the comparison of Figures 3 and 5, this can be the reason for significantly stronger "defect" phonon peak at 331 cm^{-1} in the spectrum measured at higher laser power. The frequency of the latter, as well as of some other peaks, is reduced by 1-2 cm^{-1} due to heating of the sample by exciting laser beam to a temperature of about 100° C (controlled by measurement of the Stokes/Antistokes intensity ratio).

The above-noted noticeable difference in the sizes of Cu^{+} and Zn^{2+} ions allows one to understand the observed in [13], improved structural quality of the Cu-poor CZTS films with increase of Zn content. Due to smaller size, Zn can effectively "heal" Cu vacancies. In the opposite situation – Cu-rich and Zn-poor – Zn vacancies can not be healed by the larger Cu^{+} ions.

5. Conclusions

The dependence of the phonon Raman spectra of CZTS thin films grown by flash evaporation of ZnS, CuS and SnS binary compounds on growth conditions has been studied. The conditions were: temperature of Mo coated glass substrate, ZnS-excess in the evaporation source and conditions of samples annealing (temperature, time at the maximum temperature and Ar pressure).

The films evaporated at a substrate temperature of 100^{o} C reveal typical Raman spectra for disordered kesterite structure. All Raman bands are significantly broadened related to lower crystalline nature, and the main A-symmetry peak at 331 cm^{-1} is significantly shifted downward with respect to the frequency in ordered kesterite, 338 cm^{-1}. However, the evaporation of the samples at higher substrate temperature of 350° C leads to a qualitative transformation of the spectra to those typical of well-ordered kesterite. The width of the phonon peaks in the Raman spectrum approaches lowest values when those samples are annealed at 450° C under Ar atmosphere. A similar qualitative transformation of the spectra occurs for samples deposited at 100^{o} C and subsequently annealed at 600^{o} C for 30 min under argon atmosphere. However, in all cases, even with very narrow main A-peak, a weak additional peak at 331 cm^{-1} appears in the spectra, which is associated with the disorder in the cation sublattice and formation of Cu_{Zn} and Zn_{Cu} antisites. Comparison of the spectra for different samples of known composition showed that the relative intensity of the defect peak 331 cm^{-1} correlates with the theoretical prediction: the formation of intrinsic defects in CZTS is enhanced under "Cu-poor, Zn-rich" conditions.

For films of "Cu-rich, Zn-poor" composition, further experimental confirmation was obtained by the enhancement of cation disorder under intense optical excitation.

Acknowledgement

This research is supported by the People Programme (Marie Curie Actions) of the European Union's Seventh Framework Program FP7/2007-2013/ under REA grant agreement 269167 (PVICOKEST), the Spanish MINECO project (KEST- PV, ENE2010-21541-C03) and the OPTEC grant. RC acknowledges financial support from Spanish MINECO within the program Ramon y Cajal (RYC-2011-08521).

References

[1] Todorov T.K, Tang J, Bag S, Gunawan O, Gokmen T, Zhu Y, Mitzi D.B, Adv. Energy Mater. 2013; 3: 34.

[2] Siebentritt S, Schorr S, Progr. in Photov: Res. and Appl. 2012; 20: 512.

[3] Walsh A, Chen S, Wei S-H, Gong X-G, Adv. Energy Mater. 2012; 2: 400.

[4] Schorr S, Hoebler H-J, Tovar M, European Journal of Mineralogy 2007; 19: 65.

[5] Schorr S, Gonzalez Aviles G, Phys. Stat. Solidi A 2009; 206: 1054.

[6] Washio T, Nozaki H, Fukano T, Motohiro T, Jimbo K, Katagiri H, J. Appl. Phys. 2011; 110 : 074511.

[7] Chen S, Yang J.H, Gong X.G , Walsh A, Wei S-H , Phys. Rev. B 2010; 81: 1.

[8] Choubrac L, Lafond A, Guillot-Deudon C, Moelo Y, Jobic S, Inorganic Chemistry 2012; 51: 3346.

[9] Lafond A, Choubrac L, Guillot-Deudon C, Deniard P , Jobic S, J. Inorganic and General Chemistry 2012; 638: 2571.

[10] Fontané X, Izquierdo-Roca V, Saucedo E, Schorr S, Yukhymchuk V.O, Valakh M.Ya, Perez-Rodríguez A, Morante J.R, J. Alloys and Compounds 2012; 539: 190.

[11] Valakh M.Ya, Kolomys O.F, Ponomaryov S.S, Yukhymchuk V.O, Babichuk I.S, Izquierdo-Roca V, Saucedo E, Perez-Rodriguez A, Morante J.R, Schorr S, Bodnar I.V , Phys. Stat. Solidi RRL 2013; 7: 258.

[12] Valakh M.Ya, Dzhagan V.M, Babichuk I.S, Fontané X, Perez-Rodriguez A, Schorr S, JETP Letters 2013; 98: 292.

[13] Espindola-Rodriguez M, Placidi M, Vigil-Galán O, Izquierdo-Roca V, Fontané X, Fairbrother A, Sylla D, Saucedo E, Perez-Rodriguez A, Thin Solid Films 2013; 535: 67.

[14] Caballero R, Izquierdo-Roca V, Merino J.M, Friedrich E.J, Climent-Font A, Saucedo E, Pérez-Rodríguez A, León M, Thin Solid Films 2013; 535: 62.

[15] Fernandes P.A, Salomé P.M.P, da Cunha A.F, J. Alloys and Compounds 2011; 509: 7600.

[16] Grossberg M, Krustok J, Raudoja J, Raadik T, J. Appl. Phys. 2012; 101: 102102.

[17] Khare A, Himmetoglu B, Johnson M, Norris D.J, Cococcioni M, Audil E.S, J. Appl. Phys. 2012; 111 : 083707.

[18] Holleman A.F, Wiberg N, Inorganic Chemistry. San Diego: Academic Press, (2001).

Figure captions.

Figure 1. Raman spectrum of as-evaporated samples F24 and F20.

Figure 2. Raman spectrum of as-evaporated sample F27.

Figure 3. Raman spectrum of sample F27 after annealing of type 3.

Figure 4. Raman spectrum of sample F20 after annealing of type 2.

Figure 5. Raman spectrum of sample F27 after annealing of type 3 measured at high laser excitation power.

Table I. Nominal conditions of the flash evaporation processes and composition of the as-evaporated thin films measured by EDX.

Sample	Nominal conditions				EDX composition						
	$T_{cruc,}$ ºC	$T_{substr,}$ ºC	ZnS excess, %	CuS defect, %	Cu, %	Sn, %	Zn, %	S, %	[Cu]/([Zn]+[Sn])	[Zn]/[Sn]	[S]/[M]
F19	1075	100	20	-	25.29	9.31	14.99	50.40	1.04	1.62	1.02
F20	1100	100	20	-	22.26	11.63	13.96	52.15	0.87	1.20	1.09
F24	1100	100	15	-	23.08	13.21	11.86	51.85	0.92	0.90	1.08
F22	1100	100	10	-	22.55	14.65	11.45	51.36	0.87	0.78	1.06
F26	1100	100	15	5	23.66	13.78	13.26	49.30	0.88	0.96	0.97
F27	1100	350	20	10	27.22	12.56	9.35	50.87	1.24	0.75	1.04

M = metals = Cu + Zn + Sn

Table II. Composition of thin films after different thermal treatments, measured by EDX.

Sample	TT**	Cu, %	Sn, %	Zn, %	S, %	[Cu]/([Zn]+[Sn])	[Zn]/[Sn]	[S]/[M]
F19	1	32.59	0.63	20.28	46.51	1.56	38.16	0.87
	2	23.97	10.50	13.00	52.54	1.02	1.24	1.11
F20	1	24.21	8.02	16.89	50.87	0.97	2.12	1.04
	2	21.64	12.14	13.52	53.25	0.82	1.11	1.14
F24	1	28.35	3.81	19.86	47.99	1.20	5.44	0.92
F22	2	22.11	12.43	11.05	54.41	0.94	0.89	1.19
F27	3	28.78	11.69	9.90	49.64	1.33	0.85	0.99

** TT: Thermal treatment:

1. Heating rate = 21º C/min, T = 600º C, t = 30 min, P_{Ar} = 100 Pa;

2. Heating rate = 21º C/min, T = 600º C, t = 30 min, P_{Ar} = 1000 Pa;

3. Heating rate = 10º C/min, T= 475º C, t = 60 min, P_{Ar} = 100 Pa.

Table III. Intensity ratio of Raman peaks at 332 cm^{-1} and 338 cm^{-1} for samples of different composition. Notations of thermal treatment are the same as in Table II.

Sample	TT	Cu-content	Zn- content	I_{332}/I_{338} ratio
F19	1	rich	rich	0.18
F19	2	stoichiom.	stoichiom.	0.09
F20	1	stoichiom.	rich	0.15
F20	2	poor	stoichiom.	0.13
F24	1	rich	rich	0.21
F27	-	rich	poor	0.10
F27	3	rich	poor	0.06

Figure 1a

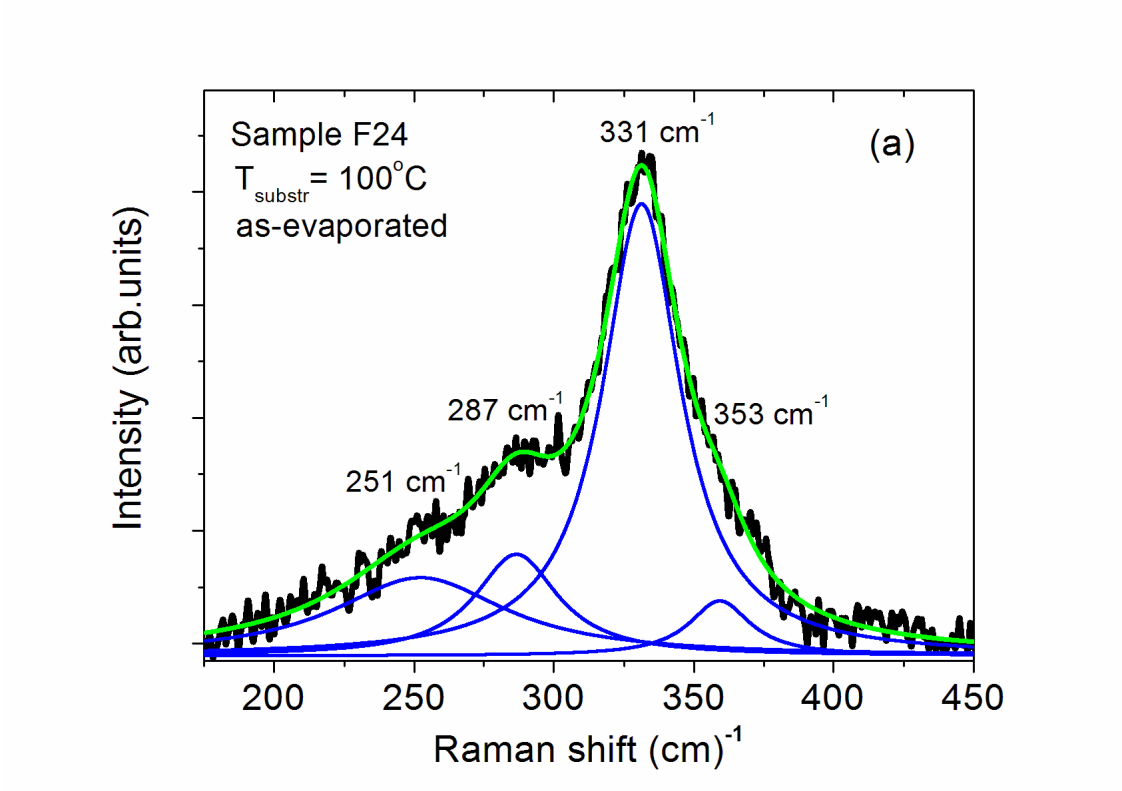

Figure 1b

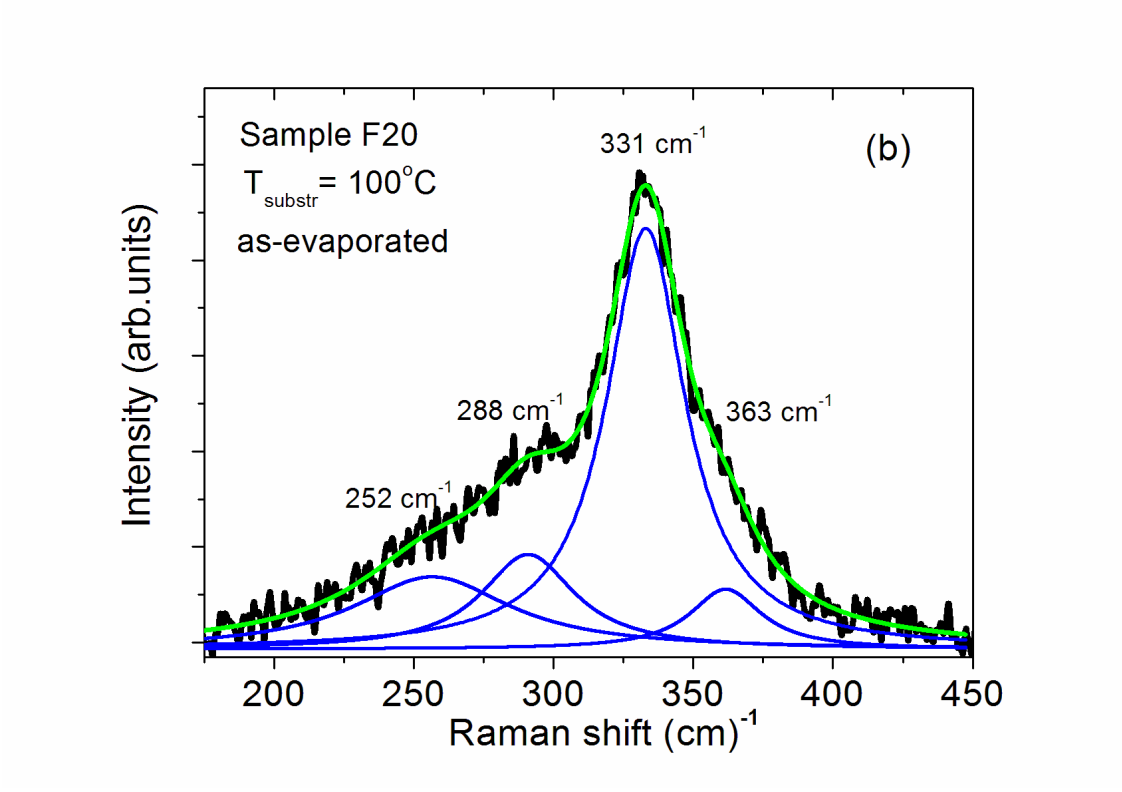

Figure 2

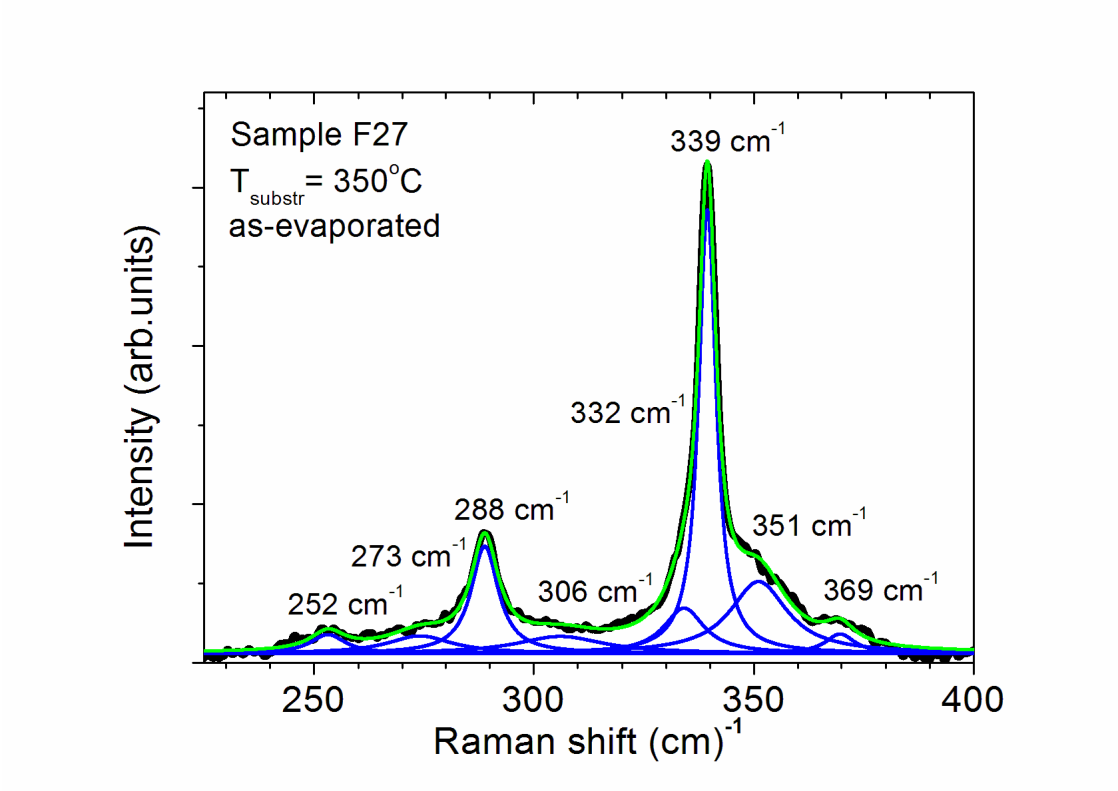
Sample F27
T substr = 350°C
as-evaporated
339 cm-1
332 cm-1
288 cm-1
273 cm-1
252 cm-1
306 cm-1
351 cm-1
369 cm-1
Intensity (arb.units)
250
300
350
400
Raman shift (cm)-1

Figure 3

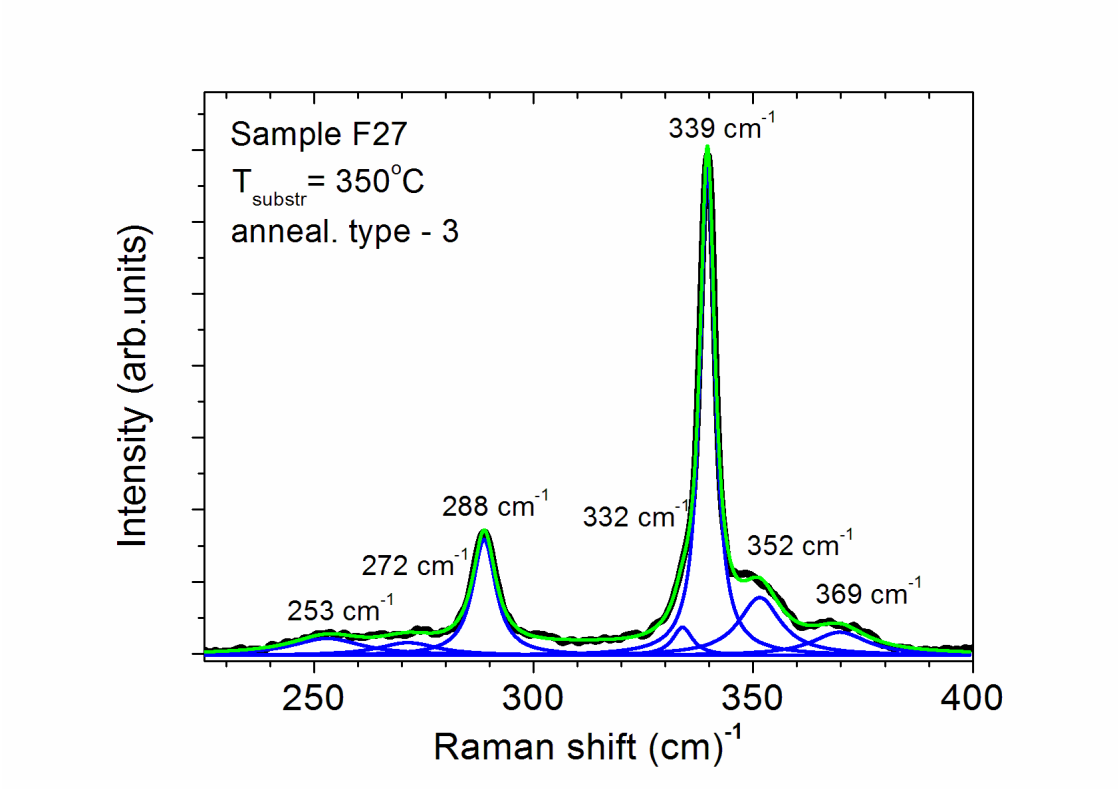
Sample F27
T substr = 350°C
anneal. type - 3
339 cm-1
288 cm-1
332 cm-1
352 cm-1
272 cm-1
369 cm-1
253 cm-1
Intensity (arb.units)
250
300
350
400
Raman shift (cm)-1

Figure 4

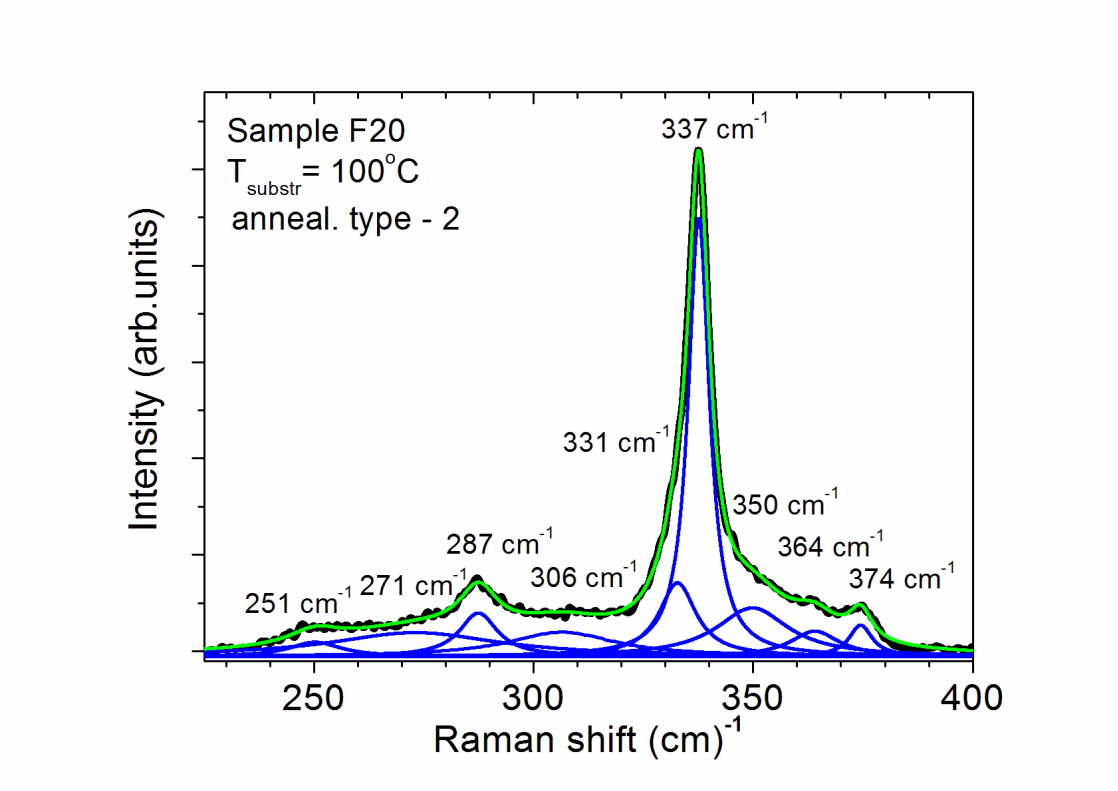
Sample F20
T substr = 100°C
anneal. type - 2
337 cm-1
331 cm-1
350 cm-1
364 cm-1
374 cm-1
287 cm-1
306 cm-1
271 cm-1
251 cm-1
Intensity (arb.units)
250
300
350
400
Raman shift (cm)-1

Figure 5

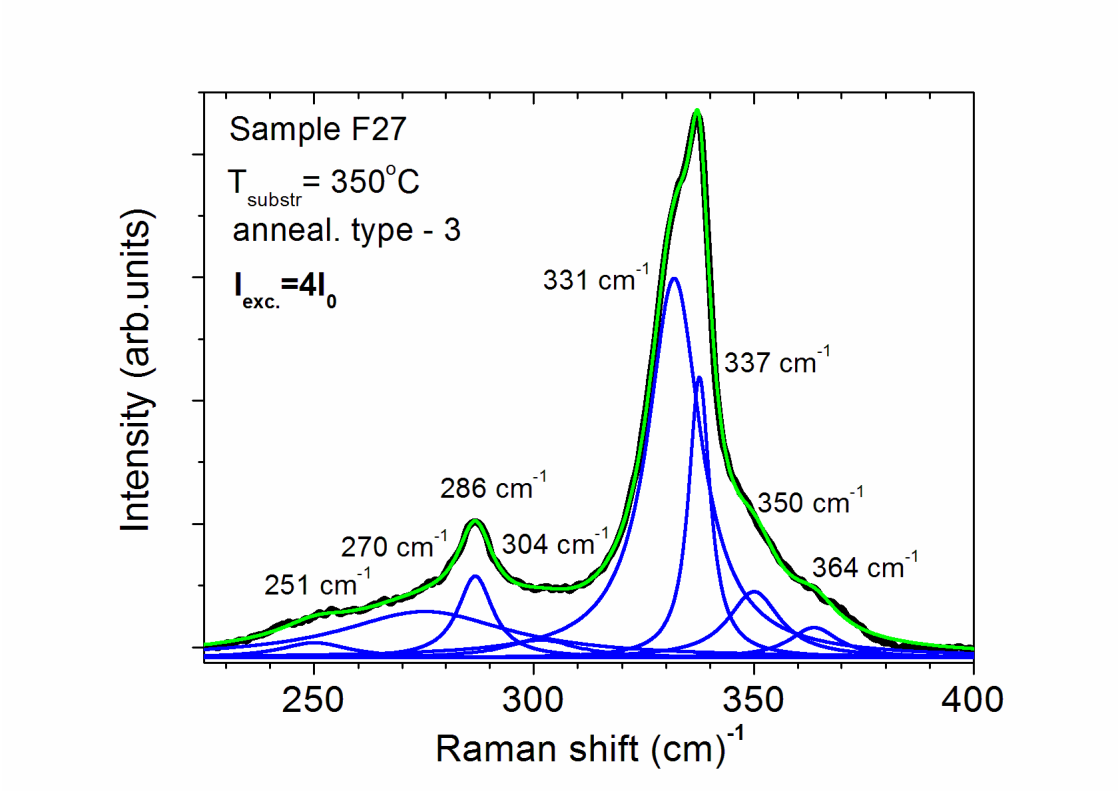
Sample F27
T substr = 350°C
anneal. type - 3
I exc. =4I 0
Intensity (arb.units)
Raman shift (cm)-1
250
300
350
400
251 cm-1
270 cm-1
286 cm-1
304 cm-1
331 cm-1
337 cm-1
350 cm-1
364 cm-1